Delayed-Input Power System Stabilizer using Supplementary Remote Signals

A. A. Hashmani, I. Erlich

ashfaque.hashmani@uni-due.de, istvan.erlich@uni-due.de
Institute of Electrical Power Systems (EAN),
University Duisburg-Essen, 47057-Duisburg, Germany

Abstract: The design of a local H_∞-based power system stabilizer controller, using wide area or global signals as additional measuring information considering time delay is presented in this paper. The wide area signals are taken from suitable remote network locations where the oscillations are well observable. A long time delay introduced by remote signal transmission and processing in wide area measurement system (WAMS), may be harmful to system stability and may degrade system robustness**.** Three methods for dealing with the effects of time delay are presented in this paper. To provide robust behavior, H_∞ control theory together with an algebraic Riccati equation approach has been applied to design the proposed controller. The simulation results show that the designed controller contributes significantly to the damping of inter-area oscillations and the enhancement of small-signal stability in the presence of uncertainty in time delay under a wide range of system operating conditions.

Keywords: inter-area oscillations, PSS, remote signals, WAMS, time delay, robust controller, H_∞ control.

1. INTRODUCTION

Weakly damped low frequency inter-area oscillations, inherent to large interconnected power systems during transient conditions, are not only dangerous for the reliability and performance of such systems but also for the quality of the supplied energy. With the heavier power transfers ahead, the damping of these oscillations will decrease unless new lines are built (construction of new lines is restricted by environmental and cost factors) or other heavy and expensive high-voltage equipment such as series-compensation is added to the grid's substations. Therefore, the achievement of maximum available transfer capability as well as a high level of power quality and security requires the need for a better coordinated protection and system stability control which leads to damping improvement.

It is found that if remote signals from one or more distant locations of the power system are applied to the controller design, the system dynamic performance can be enhanced for a better damping of inter-area oscillations (Snyder et al., 2000). The recent advances in wide area measurement (WAM) technologies using phasor measurement units (PMUs) can deliver synchronous control signals at high speed (Heydt et al., 2001). PMUs are deployed at strategic locations on the grid to obtain a coherent picture of the entire network in real time (Heydt et al., 2001). Global positioning system (GPS) technology ensures proper time synchronization among several global signals (Heydt et al., 2001). The measured global signals are then transmitted via modern telecommunication equipment to the controllers.

An experimental research (Naduvathuparambil et al., 2002) has shown that time delays in wide area control systems caused by different communication links are different but all the delays are more than 100 ms. In the case of satellite link, the propagation delay could be as high as above 700 ms. There could be a larger delay when a large number of signals are to be routed and signals from different areas are waiting for synchronization. Such large time delays can invalidate many controllers that work well in no delayed-input systems and even cause disaster accidents (Kolmanovskii et al., 1999). The design of a controller, therefore, must take into account this delay in order to provide a controller that is robust, not only for the range of operating conditions desired, but also for the uncertainty in delay (Snyder et al., 2000).

The design of a local power system stabilizer (PSS) controller using remote signals as supplementary inputs without considering time delay is presented in (Hashmani and Erlich, 2008). This paper considers a problem of improving the performance of local conventional PSS by using instantaneous measurements from remote locations of the grid considering time delay. Three methods for dealing with the effects of time delay are presented in this paper. First, time delay compensation method using lead/lag compensation along with gain scheduling for compensating effects of constant delay is presented. In the second method, Pade approximation approach is used to model time delay. The time delay model is then merged into delay-free power system model to obtain the delayed power system model. Delay compensation and Pade approximation methods deal with constant delays and are not robust regarding time delays. Time delay uncertainty is, therefore, taken into account using linear fractional transformation (LFT) method.

H_∞-based robust control technique is used to design proposed PSS controller. Digital simulation studies on a two-machine power system are conducted to investigate the effectiveness of the proposed controller during system disturbances.

The rest of the paper is organized as follows: In Section 2, design of time delay compensator, Pade approximation method to describe time delay, power system model with time delay and LFT method to describe uncertainty in time delay are presented. In Section 3, the proposed robust H_∞-based PSS controller is designed. In Section 4, a dynamic model of the two-machine system used in this study is discussed. The digital simulation results are presented in Section 5 and the conclusions are discussed in Section 6.

2. TIME DELAY IN POWER SYSTEMS

2.1 Design of Delay Compensator

Delay compensator consisting of lead/lag and gain modules is designed to diminish the effect of time delay. The effect of time delay on an oscillatory mode (σ+jω) is to introduce a phase lag with respect to angular frequency ω and gain amplification with respect to damping σ. The effect might derive eigen values of system matrix to undesirable places on complex plane and can make power system unstable. Phase lag φ due to delay τ is $\varphi = \omega\,\tau$ while the gain amplification γ_c due to delay τ is $\gamma_c = e^{-\sigma\tau}$.

Delay in time could be compensated in phase provided by lead/lag compensation block along with gain scheduling as shown in Fig. 1. In Fig. 1, output signals $\mathbf{Y}_{1df}$ of the delay-free system plant $P(s)$ are the remote input signals of the PSS controller. The time delay, therefore, occurs only in $\mathbf{Y}_{1df}$. In order to compensate the effect of this time delay on the system performance, $\mathbf{Y}_{1df}$ are added to the delay compensator $H_c(s)$. The output signals $\mathbf{Y}_{1d}$ of delay compensator, therefore, represents the delayed remote input signals of the PSS controller $\mathbf{C}(s)$. The output signal Y_{2df} of delay-free system plant is the local input signal to the PSS controller and is, therefore, without time delay.

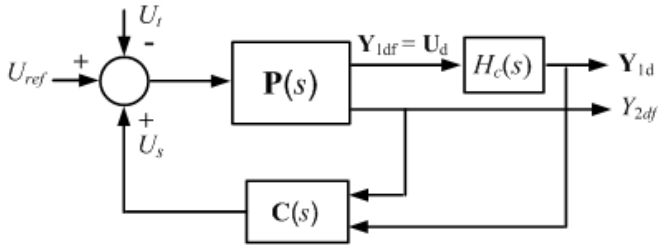

Fig. 1. Framework of wide area damping control

Transfer function of delay compensator is given as:

$$H_c(s) = K[(1 + s\,T_1)/(1 + s\,T_2)]^2$$

where, $T_1 = 1/(\omega\sqrt{\alpha})$, $T_2 = \alpha T_1$,

$$\alpha = [1 - \sin(\phi/2)]/[1 + \sin(\phi/2)],\ K = \beta e^{\sigma\tau}, 0 \prec \beta \prec 1$$

Phase lead ($\varphi = \omega\,\tau$) provided by delay compensator balances the phase lag due to delay τ. Gain K provided by delay compensator reduces the gain amplification γ_c due to delay τ.

2.2 Pade Approximation Method for Constant Delay

Time delay τ in a signal can be expressed as $e^{-s\tau}$. By using Pade approximation (Cabannes H., 1976), $e^{-s\tau}$ is expressed as (Wu Hongxia et al., 2002):

$$\dot{\mathbf{x}}_d(t) = \mathbf{A}_d\mathbf{x}_d(t) + \mathbf{B}_d\mathbf{u}_d(t) \tag{1}$$

$$\mathbf{y}_{1d}(t) = \mathbf{C}_d\mathbf{x}_d(t) + \mathbf{D}_d\mathbf{u}_d(t) \tag{2}$$

Delay-free power system plant can be expressed as follows:

$$\dot{\mathbf{x}}_{df}(t) = \mathbf{A}_{df}\mathbf{x}_{df}(t) + \mathbf{B}_{df}\mathbf{u}(t) \tag{3}$$

$$\mathbf{y}_{df}(t) = \mathbf{C}_{df}\mathbf{x}_{df}(t) + \mathbf{D}_{df}\mathbf{u}(t) \tag{4}$$

where,

$$\mathbf{y}_{df}(t) = \begin{bmatrix}\mathbf{y}_{1df} & y_{2df}\end{bmatrix}^T, \mathbf{C}_{df} = \begin{bmatrix}\mathbf{C}_{1df} & \mathbf{C}_{2df}\end{bmatrix}^T,$$

$$\mathbf{D}_{df} = \begin{bmatrix}\mathbf{D}_{1df} & \mathbf{D}_{2df}\end{bmatrix}^T.$$

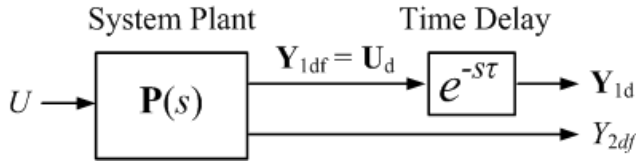

Fig. 2. Delayed-input system

In the delayed-input system shown in Fig. 2, since output signals $\mathbf{Y}_{1df}$ of delay-free block are the inputs of time delay block, i-e., $\mathbf{Y}_{1df}$=$\mathbf{U}_d$, therefore, replacement of $\mathbf{u}_d(t)$ by $\mathbf{y}_{1df}(t)$ in (1) and (2) and then substitution of the value of $\mathbf{y}_{1df}(t)$ from (4) into (1) and (2) yields:

$$\dot{\mathbf{x}}_d(t) = \mathbf{A}_d\mathbf{x}_d(t) + \mathbf{B}_d(\mathbf{C}_{1df}\mathbf{x}_{df}(t) + \mathbf{D}_{1df}\mathbf{u}(t)) \tag{5}$$

$$\mathbf{y}_{1d}(t) = \mathbf{C}_d\mathbf{x}_d(t) + \mathbf{D}_d(\mathbf{C}_{1df}\mathbf{x}_{df}(t) + \mathbf{D}_{1df}\mathbf{u}(t)) \tag{6}$$

Equations (3), (5) and (6), in matrix form, can be written as:

$$\begin{bmatrix}\dot{\mathbf{x}}_{df}(t)\\ \dot{\mathbf{x}}_d(t)\end{bmatrix} = \begin{bmatrix}\mathbf{A}_{df} & 0\\ \mathbf{B}_d\mathbf{C}_{1df} & \mathbf{A}_d\end{bmatrix}\begin{bmatrix}\mathbf{x}_{df}(t)\\ \mathbf{x}_d(t)\end{bmatrix} + \begin{bmatrix}\mathbf{B}_{df}\\ \mathbf{B}_d\mathbf{D}_{1df}\end{bmatrix}\mathbf{u}(t) \tag{7}$$

$$\mathbf{y}_{1d}(t) = \begin{bmatrix}\mathbf{D}_d\mathbf{C}_{1df} & \mathbf{C}_d\end{bmatrix}\begin{bmatrix}\mathbf{x}_{df}(t)\\ \mathbf{x}_d(t)\end{bmatrix} + \mathbf{D}_d\mathbf{D}_{1df}\mathbf{u}(t) \tag{8}$$

Equation (7) is the state equation. As the delayed-input system in Fig. 2 also has a delay free output Y_{2df}, therefore, output equation for the delayed-input system becomes:

$$\begin{bmatrix}\mathbf{y}_{1d}(t)\\ y_{2df}(t)\end{bmatrix} = \begin{bmatrix}\mathbf{D}_d\mathbf{C}_{1df} & \mathbf{C}_d\\ \mathbf{C}_{2df} & 0\end{bmatrix}\begin{bmatrix}\mathbf{x}_{df}(t)\\ \mathbf{x}_d(t)\end{bmatrix} + \begin{bmatrix}\mathbf{D}_d\mathbf{D}_{1df}\\ \mathbf{D}_{2df}\end{bmatrix}\mathbf{u}(t) \tag{9}$$

where,

$$\mathbf{A} = \begin{bmatrix}\mathbf{A}_{df} & 0\\ \mathbf{B}_d\mathbf{C}_{1df} & \mathbf{A}_d\end{bmatrix}, \mathbf{B} = \begin{bmatrix}\mathbf{B}_{df}\\ \mathbf{B}_d\mathbf{D}_{1df}\end{bmatrix},$$

$$\mathbf{C}=\begin{bmatrix}\mathbf{D}_{\mathrm{d}}\mathbf{C}_{1\mathrm{df}} & \mathbf{C}_{\mathrm{d}}\\ \mathbf{C}_{2\mathrm{df}} & 0\end{bmatrix},\ \mathbf{D}=\begin{bmatrix}\mathbf{D}_{\mathrm{d}}\mathbf{D}_{1\mathrm{df}}\\ \mathbf{D}_{2\mathrm{df}}\end{bmatrix}.$$

2.3 LFT Method for Time Delay Uncertainty

In LFT method, a time delay uncertainty can be described by an LFT (Zhou and Doyle, 1998). Delay-free power system model is then cascaded with uncertain time delay model to obtain the uncertain delayed power system model as shown in Fig. 3. Controller design based on LFT can keep the system stable over the delay uncertainty range.

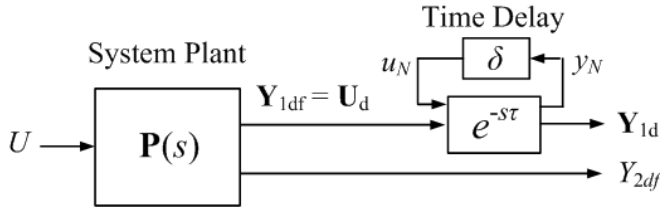

Fig. 3. Delayed-input system with LFT included

By using 1st-order Pade approximation, delay $e^{-s\tau}$ in a signal can be represented by the following equations (Wu Hongxia, et al., 2002):

$$\dot{x}_d(t)=-\frac{2}{\tau}x_d(t)+u_d(t) \tag{10}$$

$$y_d(t)=\frac{4}{\tau}x_d(t)-u_d(t) \tag{11}$$

By using (10) and (11), the block diagram of time delay $e^{-s\tau}$ can be drawn as shown in Fig. 4.

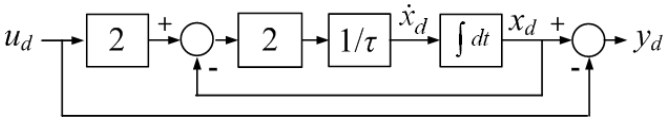

Fig. 4. Block diagram of time delay $e^{-s\tau}$

Parameter τ is not known exactly. However, it can be assumed that its value is within certain known interval, i.e.,

$$\tau=\bar{\tau}(1+p_\tau\delta_\tau) \tag{12}$$

where, $\bar{\tau}$ is the nominal value of τ. p_τ and δ_τ represent the possible (relative) perturbations on τ. p_τ represents the boundary values within which the value of τ lies. Perturbation δ_τ is assumed to be unknown but lie in the interval [-1, 1].

The term $1/\tau$ in Fig. 4 can be represented as an LFT in δ_τ, i.e., as a feedback interconnection of a constant matrix and an uncertainty matrix δ_τ, as follows:

$$\frac{1}{\tau}=\frac{1}{\bar{\tau}(1+p_\tau\delta_\tau)}=\frac{1}{\bar{\tau}}-\frac{p_\tau}{\bar{\tau}}\delta_\tau(1+p_\tau\delta_\tau)^{-1}=F_u(M_\tau,\delta_\tau) \tag{13}$$

where,

$$M_\tau=\begin{bmatrix}p_\tau & 1\\ -\dfrac{p_\tau}{\bar{\tau}} & \dfrac{1}{\bar{\tau}}\end{bmatrix} \tag{14}$$

Equation (13) together with (14) represents LFT of the term $1/\tau$. The term $1/\tau$ in Fig. 4 is, therefore, replaced by its LFT with an associated matrix M_τ, as shown in Fig. 5.

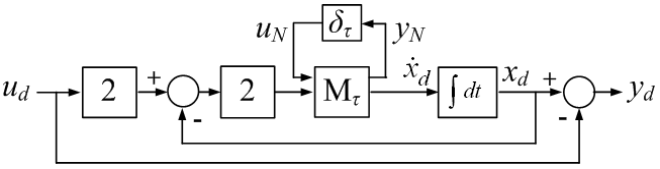

Fig. 5. Block diagram representation of time delay $e^{-s\tau}$

The block diagram shown in Fig. 5, representing delay $e^{-s\tau}$ can be described by the following equations:

$$\begin{bmatrix}y_N\\ \dot{x}_d\end{bmatrix}=\begin{bmatrix}M_{11} & M_{12}\\ M_{21} & M_{22}\end{bmatrix}\begin{bmatrix}u_N\\ 4u_d-2x_d\end{bmatrix} \tag{15}$$

$$u_N=\delta y_N \tag{16}$$

$$y_d=x_d-u_d \tag{17}$$

By substituting values of M_{11}, M_{12}, M_{21}, M_{22} from (14) into (15) and then writing (15) and (17) in matrix form, gives:

$$\begin{bmatrix}\dot{x}_d\\ y_N\\ y_d\end{bmatrix}=\begin{bmatrix}\dfrac{-2}{\bar{\tau}} & -\dfrac{p_\tau}{\bar{\tau}} & \dfrac{4}{\bar{\tau}}\\ -2 & p_\tau & 4\\ 1 & 0 & -1\end{bmatrix}\begin{bmatrix}x_d\\ u_N\\ u_d\end{bmatrix} \tag{18}$$

3. H_∞ CONTROLLER DESIGN FOR POWER SYSTEMS

3.1 Problem Formulation

The overall extended system equations for the linear, time-invariant, continuous-time composite system, composed of N subsystems, are written as follows (Hashmani and Erlich, 2008):

$$\dot{\tilde{\mathbf{x}}}(t)=\mathbf{A}_{\mathrm{cl}}\tilde{\mathbf{x}}(t)+\mathbf{B}_{\mathrm{cl}}\mathbf{w}(t) \tag{19}$$

$$\mathbf{z}(t)=\mathbf{C}_{\mathrm{cl}}\tilde{\mathbf{x}}(t)+\mathbf{D}_{\mathrm{cl}}\mathbf{w}(t) \tag{20}$$

where, $\tilde{\mathbf{x}}(t)=\begin{bmatrix}\mathbf{x}^{\mathrm{T}}(t) & \mathbf{x}_{\mathrm{c}}^{\mathrm{T}}(t)\end{bmatrix}^{\mathrm{T}}$, $\mathbf{A}_{\mathrm{cl}}=\tilde{\mathbf{A}}+\tilde{\mathbf{B}}_2\mathbf{K}_{\mathrm{D}}\tilde{\mathbf{C}}_2$,

$\mathbf{B}_{\mathrm{cl}}=\tilde{\mathbf{B}}_1+\tilde{\mathbf{B}}_2\mathbf{K}_{\mathrm{D}}\tilde{\mathbf{C}}_2$, $\mathbf{C}_{\mathrm{cl}}=\tilde{\mathbf{C}}_1+\tilde{\mathbf{D}}_{12}\mathbf{K}_{\mathrm{D}}\tilde{\mathbf{C}}_2$, $\mathbf{D}_{\mathrm{cl}}=\tilde{\mathbf{D}}_{11}+\tilde{\mathbf{D}}_{12}\mathbf{K}_{\mathrm{D}}\tilde{\mathbf{D}}_{21}$

3.2 Controller design using Riccati-based approach

Designing an H_∞ controller for the system is equivalent to that of finding matrix $\mathbf{K}_{\mathrm{D}}$, in (19) and (20), that satisfies an H_∞ norm bound condition on closed loop transfer functions $\mathbf{T}_{\mathbf{zw}}(s)=\mathbf{C}_{\mathrm{cl}}(s\mathbf{I}-\mathbf{A}_{\mathrm{cl}})^{-1}\mathbf{B}_{\mathrm{cl}}$ from disturbance $\mathbf{w}(t)$ to controlled outputs $\mathbf{z}(t)$ in Fig. 6, i.e., $\left\|\mathbf{T}_{\mathbf{zw}}(s)\right\|_\infty<\gamma$ (for a given scalar

constant $\gamma > 0$). Moreover, $\mathbf{T}_{zw}(s)$ must be stable (Gahinet and Apkarian, 1994). An algebraic Riccati equation (ARE) approach (Doyle et al., 1989) can be applied to establish the existence of control strategy.

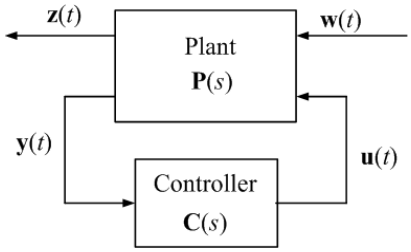

Fig. 6. General LFT framework representing general interconnected system

4. POWER SYSTEM SIMULATION MODEL

Fig. 7 shows a test two-machine power system example that is selected to apply the control design approach presented in the previous section and to illustrate the effectiveness of the proposed robust H_∞-based PSS controller for a better damping of system oscillations. Detailed information about this test system including the controllers and their parameter values can be found in (Hashmani and Erlich, 2008). Moreover, for all simulation studies as well as for the PSS design, the structure of the ith-generator together with an n_{ci}th-order PSS controller in a multimacine power system (Hashmani and Erlich, 2008) is considered.

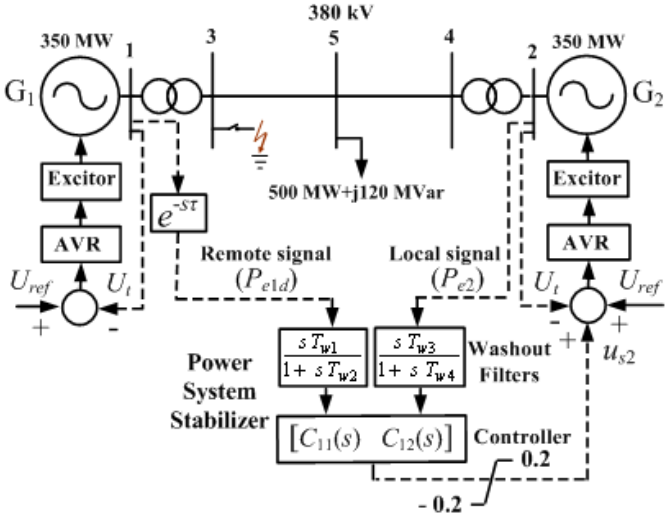

Fig. 7. One line diagram of two-machine power system together with the structure of generators and PSS

4.1 Implementation

The base operating conditions are taken from (Hashmani and Erlich, 2008). $u_1(t)$ and $u_2(t)$ are control inputs to generators G_1 and G_2 respectively. As in the considered two-machine power system of Fig. 7, PSS is located at only generator G_2, therefore, $u_1(t)$=0 and $u_2(t)$=$u_{s2}(t)$. Electrical power output of generator G_1, $P_{e1d}(t)$, is the remote measured feedback signal to the PSS which is located at the generator G_2 while electrical power output of generator G_2, $P_{e2}(t)$, is the local measured feedback signal to the PSS. Feedback input signals of the controller are $\mathbf{y}(t)$=$[P_{e1d}(t) \quad P_{e2}(t)]^T$. Electrical power output signals from both generators, the output of the PSS together with the terminal voltage error signals, which are the inputs to the regulator of the exciter, are used as regulated signals within this design framework, i.e., $\mathbf{z}(t)$=$[P_{e1d}(t) \quad P_{e2}(t) \quad u_{s2}(t)]^T$. Constant matrices $\mathbf{A}_{df}$, $\mathbf{B}_{11df}$, $\mathbf{B}_{12df}$, $\mathbf{B}_{21df}$, $\mathbf{B}_{22df}$, $\mathbf{C}_{11df}$, $\mathbf{C}_{12df}$, $\mathbf{C}_{21df}$, $\mathbf{C}_{22df}$, $\mathbf{D}_{111df}$, $\mathbf{D}_{112df}$, $\mathbf{D}_{121df}$, $\mathbf{D}_{122df}$, $\mathbf{D}_{211df}$, $\mathbf{D}_{212df}$ for the considered two machine system can be found in (Hashmani and Erlich, 2008).

The design procedure of Section 3.2 is used to design the controller. Matlab Robust Control Tool box is used for the design purpose.

4.2 Reduced-Order Controller Design for Delay-Free System

H_∞-based PSS controller for delay-free system is (Hashmani and Erlich, 2008):

$$\left[11.714\frac{1+s\,0.004}{1+s\,0.0501} \qquad 14.999\frac{1+s\,0.007}{1+s\,0.0501}\right]$$

With this controller H_∞ disturbance attenuation is $\gamma = 0.0101$.

4.3 Design of Delay Compensator for Constant Delay System

By considering that the time delay in the remote input signal $P_{e1d}(t)$ of the PSS controller is 700 ms and following the procedure described in Section 2.1, delay compensator designed is: $0.1[(1+s\,0.8469)/(1+s\,0.0749)]^2$

4.4 Controller Design for Constant Delay System

By considering that the time delay is 700 ms and using 1st-order Pade approximation, the constant matrices A_d, B_d, C_d, D_d for the time delay model of (1) and (2) can be obtained as:

$$A_d = -\frac{2}{\tau} = -\frac{2}{0.8},\ B_d = 1,\ C_d = \frac{4}{\tau} = \frac{4}{0.8},\ D_d = -1$$

For reducing the order of controller, the procedure given in (Hashmani and Erlich, 2008) is followed. The reduced-order H_∞-based PSS controller, thus, obtained is:

$$\left[4.613\frac{1+s\,14.71}{1+s\,28.59} \qquad 5.2983\frac{1+s\,11.85}{1+s\,28.59}\right]$$

The H_∞ disturbance attenuation is $\gamma = 0.0102$.

4.5 Controller Design for Uncertain Delay System

By considering that the uncertainty in the time delay ranges from 0 ms to 700 ms, (12) can be written as:

$$\tau = \bar{\tau} + \bar{\tau} p_\tau \delta_\tau = 0.35 + 0.35\delta_\tau$$

where, $\bar{\tau} = 0.35\,\text{s}$, p_τ=1 and $\delta_\tau \in [-1,1]$.

By substituting the values of $\bar{\tau}$ and p_τ into (22), the constant matrices A_d, B_d, C_d, D_d, for the uncertain time delay model of (10) and (11), can be obtained as follows:

$$A_d = -5.7142, B_d = 11.4284, C_d = 1, D_d = -1$$

Reduced-order H_∞-based PSS controller, thus, obtained is:

$$\left[32.19\frac{1+s0.031}{1+s\,3.264} \qquad 25.456\frac{1+s\,0.47}{1+s3.264}\right]$$

The H_∞ disturbance attenuation is $\gamma = 0.6228$.

5. SIMULATION RESULTS

In order to simulate the system behaviour under large disturbance conditions, a balanced three-phase fault is applied at bus 3 as shown in Fig. 7. The fault sequence of the three-phase fault used in these simulations is as follows:

Stage 1: The system is in pre-fault steady-state.

Stage 2: A three-phase fault occurs at t = 1.0 s.

Stage 3: The fault is cleared at t = 1.2 s.

Stage 4: The system is in a post-fault state.

5.1 Delay Compensator Case

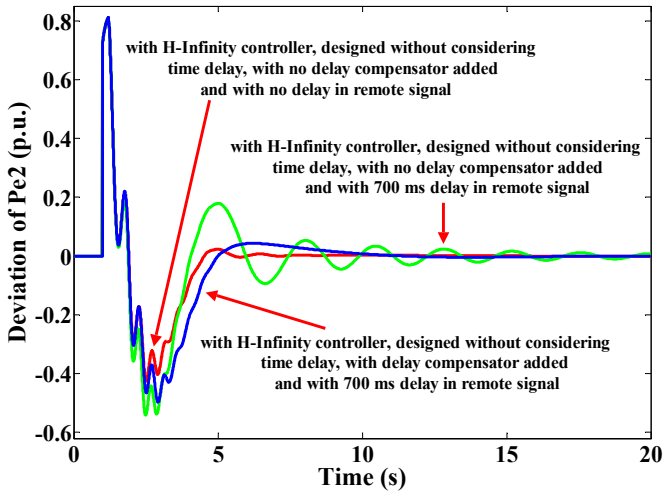

Fig. 8. Deviation of P_{e2} following a three-phase fault with H_∞ controller designed without considering time delay and with and without delay compensator added

Fig. 8 shows the behaviours of deviation of $P_{e2}(t)$ with H_∞-based PSS controller designed without considering delay in its remote input signal. Fig. 8 indicates that the response of deviation of $P_{e2}(t)$, with H_∞-based PSS controller designed without considering time delay, is better damped when no delay is included in the remote input signal of the controller during the simulation but becomes oscillatory when a constant delay of 700 ms is included in the remote input signal during the simulation. Fig. 8 also indicates that for a constant delay of 700 ms included in the remote input signal during the simulation, the response of deviation of $P_{e2}(t)$ is better damped with the same H_∞-based PSS controller, designed without considering delay, when cascaded with the delay compensator designed for the delay of 700 ms.

5.2 Pade Approximation Method for Constant Delay Case

Fig. 9 shows the behaviours of deviation of $P_{e2}(t)$ with H_∞-based PSS controllers designed without considering time delay and with considering constant time delay of 700 ms in their remote input signals. Fig. 9 indicates that for a constant delay of 700 ms included in the remote input signal during the simulation, the response of deviation of $P_{e2}(t)$, with H_∞-based PSS controller redesigned considering constant delay of 700 ms, is better damped as compared to that with H_∞-based PSS controller designed without considering delay.

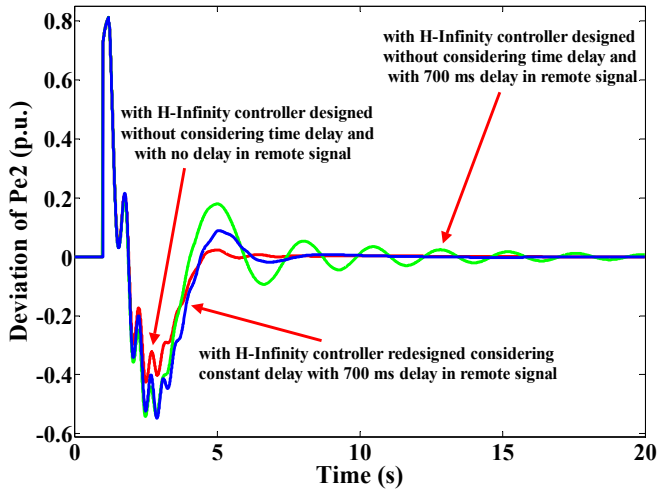

Fig. 9. Deviation of P_{e2} following a three-phase fault with H_∞ controller designed without considering time delay and with H_∞ controller redesigned considering constant delay

5.3 LFT Method for Time Delay Uncertainty Case

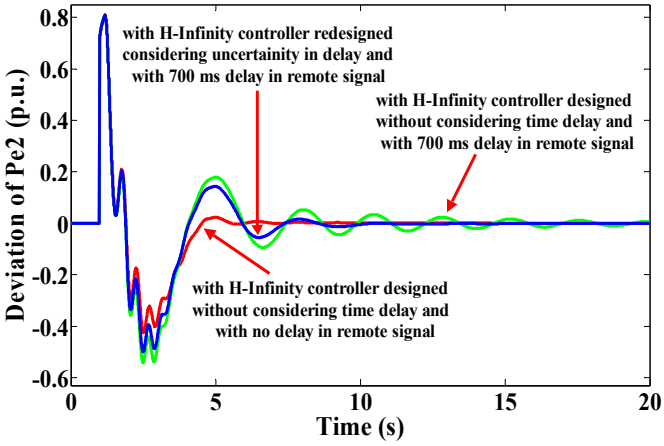

Fig.10. Deviation of P_{e2} following a three-phase fault with H_∞ controller designed without considering time delay and with H_∞ controller redesigned considering delay uncertainty

Fig. 10 shows the behaviours of deviation of $P_{e2}(t)$ with H_∞-based PSS controllers designed without considering time

delay and with considering uncertainty in the time delay in its remote input signal. Fig. 10 indicates that for a time delay of 700 ms included in the remote input signal during the simulation, the response of deviation of $P_{e2}(t)$, with the H_∞-based PSS controller redesigned considering uncertainty in time delay, is better damped as compared to that with the H_∞-based PSS controller designed without considering delay.

5.4 Robustness of Controller Regarding Time Delay

To further assess effectiveness of the proposed approach regarding robustness, transient performance indices are computed for different time delays. Transient performance index for electrical power output of the generator, following a three-phase short-circuit of 200 ms duration at bus 3 in Fig. 7, is computed using the following equation:

$$I = \int_0^t \left| P_e(t) - P_{e0}(t) \right| \quad dt \tag{21}$$

For comparison purpose, this index is normalized to the index for the mean value of delay range considered in the delay uncertainty case:

$$I_N = \frac{I_{DD}}{I_{MD}} \tag{22}$$

where I_{DD} is transient performance index for different time delays and I_{MD} is transient performance index for the mean value of delay range considered in the delay uncertainty case.

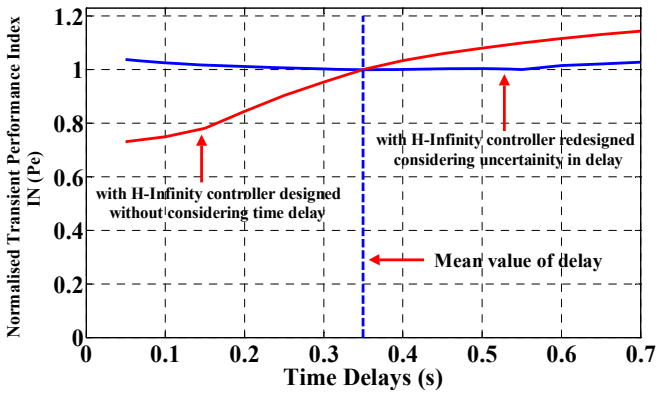

Fig.11. Normalized transient performance index I_N for electrical power generated

The normalized transient performance indices for the electrical power output of the generator, for the time delays ranging from 0 to 700 ms, with the proposed H_∞-based PSS controller, designed considering uncertainty in delay in its remote input signal and with the H_∞-based PSS controller, designed without considering delay in its remote input signal are shown in Fig. 11. It can be seen from the Fig. 11 that the normalized transient performance indices for the proposed H_∞-based PSS controller, are more near to unity, for the range of delays for which the controller is designed, as compared to those for the H_∞-based PSS controller designed without considering delay in its remote input signal. This clearly indicates that, for different delays, the transient responses of the generator with the proposed H_∞-based PSS controller, designed considering delay uncertainty, are well damped as compared to those with the H_∞-based PSS controller, designed without considering delay. This indicates that, the system behavior exhibits robustness with the proposed controller for the range of delays for which the controller is designed. This shows that the proposed H_∞-based PSS controller, designed considering delay uncertainty, is more robust regarding time delay uncertainty as compared to the H_∞-based PSS controller, designed without considering delay.

6. CONCLUSIONS

An H_∞-based dynamic output feedback PSS controller design, using both local and remote signals as the feedback input signals, considering time delay in the remote signals, is developed. Three methods for dealing with the effects of time delay are presented. The nonlinear simulations results have shown that the proposed controller is effective and robust in suppressing system oscillations not only for a wide range of operating conditions but also for the uncertainty in delay under large disturbances in the system studied.

REFERENCES

Cabannes H. (1976). *Pade approximations method and its applications to mechanics*, Springer-Verlag, New York.

Doyle John C., Glover Keith, Khargonekar Pramod P., and Francis Bruce A. (1989). State-space solutions to standard H_2 and H_∞ control problems. *IEEE Transactions on Automatic Control,* vol. 34, No. 8, pp. 831–847.

Gahinet P. and Apkarian P. (1994). A linear matrix inequality approach to H_∞ control. *International Journal of Robust and Nonlinear control*, vol. 4, pp. 421-448.

Hashmani A. A., Erlich I. (2008). Power system stabilizer by using supplementary remote signals. *PSCC*.

Heydt G. T., Liu C. C., Phadke A. G., and Vittal V. (2001). Solutions for the crisis in electric power supply. *IEEE Computer Applications in Power*, pp. 22-30.

Kolmanovskii V. B., Niculescu S. I., and Gu K. (1999). Delay effects on stability: a survey. *38th IEEE Conference on Decision and Control*, pp. 1993-1998.

Naduvathuparambil B., Valenti M. C., and Feliachi A. (2002). Communication delays in wide area measurement systems. *34th Southeastern Symposium on System Theory*, pp. 118-122.

Snyder Aaron F., Ivanescu Dan, HadjSaid Nouredine, Geroges Didier, and Margotin Thibault (2000). Delay-input wide-area stability control with synchronized phasor measurements. *IEEE PES Summer Meeting,* vol. 2, pp. 1009-1014.

Wu Hongxia, Ni Hui, and Heydt G. T. (2002). The impact of time delay on robust control design in power systems. *IEEE Power Engineering Society Winter Meeting,* vol. 2, pp. 1511–1516.

Zhou Kemin, and Doyle John C. (1998). *Essentials of robust control*, Prentice Hall, Upper Saddle River, New Jersey.